Acknowledgment

The author wishes to thank Prof. M. Hashimoto of Osaka Electro-Communication University who motivated this work.

References

[1] D. Gloge, "Weakly guiding fibers," *Appl. Opt.*, vol. 10, no. 10, pp. 2252–2258, Oct. 1971.

[2] K. Morishita, Y. Obata, and N. Kumagai, "An exact analysis of group velocity for propagation modes in optical fibers," *IEEE Trans. Microwave Theory Tech.*, vol. MTT-30, pp. 1821–1826, Nov. 1982.

[3] E. Snitzer, "Cylindrical dielectric waveguide modes," *J. Opt. Soc. Amer.*, vol. 51, no. 5, pp. 491–498, May 1961.

[4] M. H. Kuhn, "The influence of the refractive index step due to the finite cladding of homogeneous fibers on the hybrid properties of modes," *Arch. Elek. Übertragung.*, vol. 28, no. 10, pp. 393–401, Oct. 1974.

[5] J. A. Arnaud, *Beam and Fiber Optics*. New York: Academic, 1976, pp. 372–374.

[6] M. Hashimoto, "Propagation of inhomogeneous waves in cladded optical fibers," *Int. J. Electron.*, vol. 46, no. 2, pp. 125–139, 1979.

[7] M. M. Z. Kharadly and J. E. Lewis, "Properties of dielectric-tube waveguides," *Proc. Inst. Elec. Eng.*, vol. 116, no. 2, pp. 214–224, Feb. 1969.

[8] A. Safaai-Jazi and G. L. Yip, "Classification of hybrid modes in cylindrical dielectric optical waveguides," *Radio Sci.*, vol. 12, no. 4, pp. 603–609, July–Aug. 1977.

[9] T. Tanaka and Y. Suematsu, "An exact analysis of cylindrical fiber with index distribution by matrix method and its application to focusing fiber," *Trans. Inst. Electron. Commun. Eng. Jap.*, vol. E59, no. 11, pp. 1–8, Nov. 1976.

[10] P. J. B. Clarricoats and K. B. Chan, "Propagation behaviour of cylindrical-dielectric-rod waveguides," *Proc. Inst. Elec. Eng.*, vol. 120, no. 11, pp. 1371–1378, Nov. 1973.

[11] H.-G. Unger, *Planar Optical Waveguides and Fibres*. Oxford: Oxford Univ. Press, 1977, p. 419.

[12] M. Hashimoto, "Hybrid modes of graded-index optical fibers," *Electron. Lett.*, vol. 17, no. 18, pp. 659–661, Sept. 1981; erratum, vol. 17, no. 25, p. 987, Dec. 1981.

[13] M. Hashimoto, "Circularly polarized modal skew rays in graded-index optical fibers," *J. Opt. Soc. Amer.*, vol. 72, no. 9, pp. 1147–1151, Sept. 1982.

[14] M. Hashimoto, "On hybrid modes in inhomogeneous optical fibers," *Tech. Rep. Inst. Electr. Eng. Jap.*, vol. EMT-81-35, pp. 15–24, Oct. 1981 (in Japanese).

[15] B. K. Garside, T. K. Lim, and J. P. Marton, "Propagation characteristics of parabolic-index fiber modes: Linearly polarized approximation," *J. Opt. Soc. Amer.*, vol. 70, no. 4, pp. 395–400, Apr. 1980.

[16] M. J. Adams, *An Introduction to Optical Waveguides*. New York: Wiley, 1981.

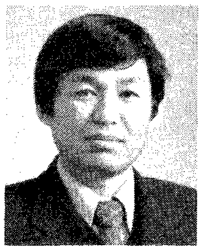

Katsumi Morishita, (S'74–M'77) was born in Fukui, Japan, on February 24, 1949. He received the B.E., M.E., and Ph.D. degrees in electrical communication engineering from Osaka University, Osaka, Japan, in 1972, 1974, and 1977, respectively.

From 1977 to 1978 he was a Postdoctoral Fellow of the Japan Society for the Promotion of Science. Since 1981 he has been with Osaka Electro-Communication University, Neyagawa-shi, Osaka, Japan, where he is now an Associate Professor in the Department of Precision Engineering. His research interests are in the areas of electromagnetic field analyses and optical waveguides.

Dr. Morishita is a member of the Institute of Electronics and Communication Engineers of Japan and the Society of Instrument and Control Engineers of Japan.

Empirical Expressions for Fin-Line Design

ARVIND K. SHARMA, MEMBER, IEEE, AND WOLFGANG J. R. HOEFER, SENIOR MEMBER, IEEE

Abstract—This paper presents empirical expressions in closed form for the design of unilateral and bilateral fin-lines. The guided wavelength and the characteristic impedance calculated with these expressions agree, typically, within ±2 percent with values obtained using numerical techniques in the normalized frequency range $0.35 \leqslant b/\lambda \leqslant 0.7$, which is suitable for most practical applications.

I. Introduction

FIN-LINES FIND frequent applications in millimeter-wave integrated-circuit design. This is attributed to their favorable properties, such as low dispersion, broad single-mode bandwidth, moderate attenuation, and compatibility with semiconductor devices. Among various possible configurations, unilateral and bilateral fin-lines are of particular interest (see Fig. 1).

To this date, the propagation characteristics of fin-lines have been obtained with various methods. An early paper by Meier [1] described the propagating mode as a variation of the dominant mode in ridged waveguide. His procedure requires a test measurement to determine the equivalent dielectric constant of the fin-line structure. This is both expensive and time consuming. The analysis procedures by Saad and Begemann [2] and Hoefer [3] are based on ridged waveguide theory, and provide only an approximate solution. On the other hand, an accurate description of propagation in fin-lines, such as presented by Hofmann [4], and

Manuscript received November 23, 1981; revised December 8, 1982.
A. K. Sharma is with the Microwave Technology Center, RCA Laboratories, David Sarnoff Research Center, Princeton, NJ 08540.
W. J. R. Hoefer is with the Department of Electrical Engineering, University of Ottawa, Ottawa, Ontario, K1N6N5, Canada.

0018-9480/83/0400-0350$01.00 ©1983 IEEE

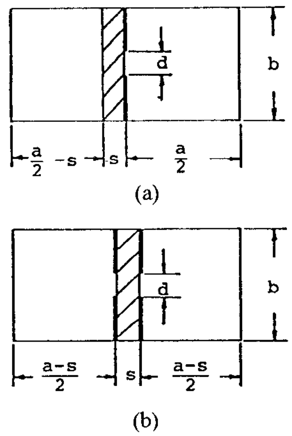

Fig. 1. Fin-line configurations. (a) Unilateral fin-line. (b) Bilateral fin-line.

recently by Knorr and Shayda [5], Schmidt and Itoh [6], and Beyer and Wolff [7], demands considerable analytical efforts and invariably leads to complicated computer programming. It is, therefore, desirable to have a design method which combines the flexibility of analytical expressions with the accuracy of numerical techniques. With this in mind, we have developed the following empirical formulas.

We believe that Meier's expressions describe the dispersion in fin-lines well enough for most practical applications. But, in order to circumvent the inconvenience of the required test measurement, we have developed empirical expressions for the equivalent dielectric constant k_e, the cutoff wavelength λ_{ca} in the equivalent ridged waveguide, as well as for the cutoff wavelength λ_{cf} in fin-lines. We present the basic approach in Section II, and the detailed empirical expressions in subsequent sections.

II. The Derivation of the Design Expressions

Meier's expressions for guided wavelength λ_g and characteristic impedance Z_0 in fin-line are [1]

$$\lambda_g = \lambda\left[k_e - (\lambda/\lambda_{ca})^2\right]^{-1/2} \tag{1}$$

and

$$Z_0 = Z_{0\infty}\left[k_e - (\lambda/\lambda_{ca})^2\right]^{-1/2} \tag{2}$$

where k_e is the equivalent dielectric constant, and λ is the free-space wavelength. λ_{ca} and $Z_{0\infty}$ are the cutoff wavelength and the characteristic impedance at infinite frequency of a ridged waveguide of identical dimensions. In Meier's expressions (1) and (2), the term k_e is regarded as a constant and is determined by a single test measurement. Strictly speaking, it characterizes a fictitious ridged waveguide uniformly filled with a dielectric of relative permittivity k_e. This first-order approximation is satisfactory only if the relative dielectric constant of the fin-line substrate is close to unity, and if the substrate occupies only a very small fraction of the guide cross section. If, however, ϵ_r is larger than 2.5, k_e must be considered frequency dependent, and we assume it to have the following general form [8]:

$$k_e = k_c \cdot F(d/b, s/a, \lambda, \epsilon_r). \tag{3}$$

k_c is the equivalent dielectric constant at cutoff given by

$$k_c = (\lambda_{cf}/\lambda_{ca})^2 \tag{4}$$

where λ_{cf} and λ_{ca} are the cutoff wavelength in the fin-line and in the equivalent ridged waveguide, respectively. The correction factor F is determined such that (1) and (2) yield the results obtained with the rigorous numerical techniques [4]–[9].

In the millimeter-wave range, standard waveguides have an aspect ratio $b/a = 1/2$. Furthermore, the substrates most frequently used in this range have a relative dielectric constant $\epsilon_r = 2.22$ (RT – Duroid) or $\epsilon_r = 3$ (Kapton). Expressions in this paper have therefore been derived for these parameters in the normalized frequency range of $0.35 \leqslant b/\lambda \leqslant 0.7$ which is suitable for most practical applications.

III. Numerical Evaluation of the Normalized Cutoff Frequencies

The accurate numerical evaluation of the normalized cutoff frequencies in fin-lines is accomplished with the hybrid mode formulation of the spectral domain technique [4], [5], [9]. In this technique, the Fourier transform of the dyadic Green's functions are related to the transform of the current densities on the conductors and the electric fields in the region complementary to the conductors, via the equation

$$\begin{bmatrix} \tilde{H}_{11}(\alpha_n,\beta,k_0) & \tilde{H}_{12}(\alpha_n,\beta,k_0) \\ \tilde{H}_{21}(\alpha_n,\beta,k_0) & \tilde{H}_{22}(\alpha_n,\beta,k_0)\end{bmatrix}\begin{bmatrix}\tilde{E}_x(\alpha_n) \\ \tilde{E}_z(\alpha_n)\end{bmatrix} = \begin{bmatrix}\tilde{J}_x(\alpha_n) \\ \tilde{J}_z(\alpha_n)\end{bmatrix} \tag{5}$$

where α_n is the Fourier-transform variable, β is the propagation constant, and k_0 is the free-space wavenumber. $\tilde{E}_x$, $\tilde{E}_z$, $\tilde{J}_x$, and $\tilde{J}_z$ are the electric fields in the aperture and the current densities on the conductors, respectively.

With the application of Galerkin's procedure and Parseval's theorem, we obtain a set of algebraic equations in terms of unknown constants of the basis functions. At cutoff, a nontrivial solution for the wavenumber k_0 is obtained by setting the determinant of the coefficient matrix equal to zero and finding the root of the equation. The numerical values for the normalized cutoff frequencies evaluated for the dielectric constants $\epsilon_r = 2.22$ and 3 are displayed in Tables I and II for unilateral and bilateral fin-lines, respectively. These values serve as a reference for other methods of fin-line analysis and are also utilized to derive the empirical expressions.

IV. Empirical Expressions for the Normalized Cutoff Frequencies

Meier's expressions require the knowledge of the cutoff wavelength λ_{ca} in an equivalent ridged waveguide, obtained by setting $\epsilon_r = 1$. However, in order to keep the analytical expressions for λ_{ca} as simple as possible, we

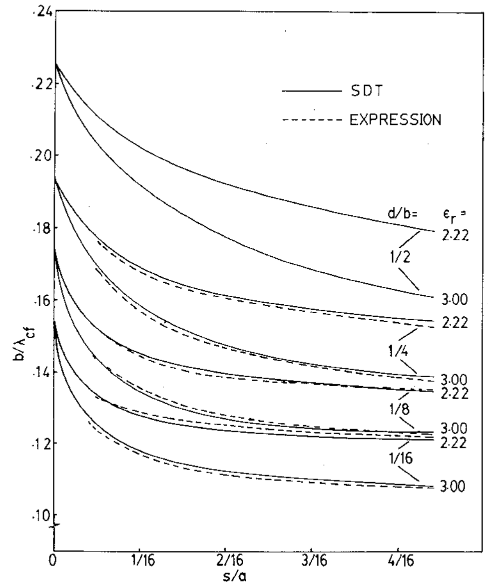

Fig. 2. Normalized cutoff frequencies in unilateral fin-lines. $b/a = 0.5$, $\epsilon_r = 2.22$ and 3.

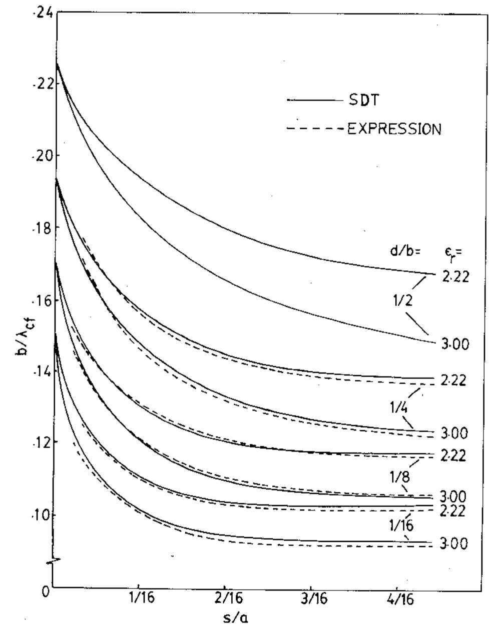

Fig. 3. Normalized cutoff frequencies in bilateral fin-lines. $b/a = 0.5$, $\epsilon_r = 2.22$ and 3.

assume that the equivalent ridged waveguide is obtained by letting the substrate thickness tend toward zero, which leads to the same expression for λ_{ca} in the unilateral and bilateral case. The normalized cutoff frequency (b/λ_{ca}) is then given by

$$b/\lambda_{ca} = 0.245(d/b)^{0.173} \tag{6}$$

which is valid for $1/16 \leqslant d/b \leqslant 1/4$ and is accurate to ± 1 percent.

For unilateral and bilateral fin-lines, the general expression for the normalized cutoff frequency (d/λ_{cf}) can be written in terms of the d/b and s/a

$$b/\lambda_{cf} = A(d/b)^p(s/a)^q. \tag{7}$$

TABLE I
NORMALIZED CUTOFF FREQUENCY b/λ_c OF THE DOMINANT MODE IN UNILATERAL FIN-LINES

Normalized Thickness s/a	Normalized Gap Width d/b	Cutoff frequency b/λ_c of the Dominant Mode, ϵ_r = 2.22, SDT	ϵ_r = 2.22, Expression	ϵ_r = 3.0, SDT	ϵ_r = 3.0, Expression
1/4	1/2	0.18070	-	0.16269	-
	1/4	0.15457	0.15340	0.13908	0.13840
	1/8	0.13505	0.13561	0.12146	0.12233
	1/16	0.12096	0.11988	0.10874	0.10814
1/8	1/2	0.19210	-	0.17706	-
	1/4	0.16140	0.16040	0.14756	0.14673
	1/8	0.13942	0.14085	0.12684	0.12800
	1/16	0.12396	0.12369	0.11244	0.11167
1/16	1/2	0.20248	-	0.19114	-
	1/4	0.16925	0.16755	0.15799	0.15640
	1/8	0.14499	0.14609	0.13410	0.13502
	1/16	0.12796	0.12738	0.11755	0.11657
1/32	1/2	0.21049	-	0.20275	-
	1/4	0.17698	0.17603	0.16881	0.16766
	1/8	0.15139	0.15283	0.14285	0.14364
	1/16	0.13286	0.13268	0.12409	0.12306

TABLE II
NORMALIZED CUTOFF FREQUENCY b/λ_c OF THE DOMINANT MODE IN BILATERAL FIN-LINES

Normalized Thickness s/a	Normalized Gap Width d/b	Cutoff frequency b/λ_c of the Dominant Mode, ϵ_r = 2.22, SDT	ϵ_r = 2.22, Expression	ϵ_r = 3.0, SDT	ϵ_r = 3.0, Expression
1/4	1/2	0.16833	-	0.15079	-
	1/4	0.13814	0.13695	0.12401	0.12292
	1/8	0.11779	0.11876	0.10576	0.10689
	1/16	0.10387	0.10298	0.09325	0.09296
1/8	1/2	0.17973	-	0.16531	-
	1/4	0.14489	0.14365	0.13254	0.13149
	1/8	0.12058	0.12154	0.10976	0.11087
	1/16	0.10409	0.10283	0.09443	0.09348
1/16	1/2	0.19279	-	0.18168	-
	1/4	0.15732	0.15577	0.14706	0.14567
	1/8	0.12955	0.13073	0.11999	0.12118
	1/16	0.11014	0.10972	0.10123	0.10082
1/32	1/2	0.20399	-	0.19623	-
	1/4	0.16925	0.16987	0.16159	0.16270
	1/8	0.14110	0.14183	0.13332	0.13409
	1/16	0.11941	0.11842	0.11160	0.11051

In the following, the unknown constants appearing in (7) are given for the range of structural parameters $1/16 \leqslant d/b \leqslant 1/4$ and $1/32 \leqslant s/a \leqslant 1/4$.

For Unilateral Fin-Lines ($\epsilon_r = 2.22$)

$$A = 0.1748$$

$$p = \begin{cases} 0.16(s/a)^{-0.07}, & 1/32 \leqslant s/a \leqslant 1/20 \\ 0.16(s/a)^{-0.07} \\ \quad -0.001\ln[(s/a)-(1/32)], & 1/20 \leqslant s/a \leqslant 1/4 \end{cases}$$

$$q = -0.0836. \tag{8}$$

For Unilateral Fin-Lines ($\epsilon_r = 3$)

$$A = 0.1495$$

$$p = \begin{cases} 0.1732(s/a)^{-0.073}, & 1/32 \leqslant s/a < 1/10 \\ 0.1453(s/a)^{-0.1463}, & 1/10 \leqslant s/a \leqslant 1/4 \end{cases}$$

$$q = -0.1223. \tag{9}$$

For Bilateral Fin-Lines ($\epsilon_r = 2.22$)

$$A = 0.15$$

$$p = \begin{cases} 0.225(s/a)^{-0.042}, & 1/32 \leqslant s/a \leqslant 1/10 \\ 0.149(s/a)^{-0.23}, & 1/10 \leqslant s/a \leqslant 1/4 \end{cases}$$

$$q = -0.14. \tag{10}$$

For Bilateral Fin-Lines ($\epsilon_r = 3$)

$$A = 0.1255$$

$$p = \begin{cases} 0.21772(s/a)^{-0.07155}, & 1/32 \leqslant s/a \leqslant 1/15 \\ 0.2907 - 0.3568(s/a), & 1/15 \leqslant s/a \leqslant 1/4 \end{cases}$$

$$q = -0.1865. \tag{11}$$

Tables I and II compare the above expressions and numerical results obtained with the spectral domain technique. Results agree within ± 1 percent, which inspires confidence in the above expressions. Figs. 2 and 3 display these results graphically.

V. Equivalent Dielectric Constant

Given the cutoff frequencies in fin-lines and ridged waveguides of identical dimensions, the equivalent dielectric constant k_c at cutoff is calculated with (3). k_e is then obtained by multiplying k_c with a correction factor F. The expressions for F are as follows.

For Unilateral Fin-Lines ($\epsilon_r = 2.22$)

$$F = \begin{cases} [1.0 + 0.43(s/a)](d/b)^{p_1}, & 1/32 \leqslant s/a \leqslant 1/8 \\ [1.02 + 0.264(s/a)](d/b)^{p_1}, & 1/8 \leqslant s/a \leqslant 1/4 \end{cases} \tag{12}$$

where

$$p_1 = 0.096(s/a) - 0.007.$$

For Unilateral Fin-Lines ($\epsilon_r = 3$)

$$F = F' + 0.25308(b/\lambda) - 0.135$$

$$F' = \begin{cases} 1.368(s/a)^{0.086}(d/b)^{p_1}, & 1/32 \leqslant s/a \leqslant 1/8 \\ [1.122 + 0.176(s/a)]^{p_2}, & 1/8 < s/a \leqslant 1/4 \end{cases} \tag{13}$$

where

$$p_1 = 0.375(s/a) - 0.0233$$

$$p_2 = 0.032 - 3.0[(s/a) - (3/16)]^2.$$

For Bilateral Fin-Lines ($\epsilon_r = 2.22$)

$$F = \begin{cases} 0.78(s/a)^{-0.098}(d/b)^{0.109}, & 1/32 \leqslant s/a < 1/8 \\ [1.04 - 0.2(s/a)](d/b)^{p_1}, & 1/8 \leqslant s/a \leqslant 1/4 \end{cases} \tag{14}$$

where

$$p_1 = 0.152 - 0.256(s/a).$$

For Bilateral Fin-Lines ($\epsilon_r = 3$)

$$F = F' + 0.08436(b/\lambda) - 0.045$$

$$F' = \begin{cases} 0.975(s/a)^{-0.026}(d/b)^{p_1}, & 1/32 \leqslant s/a < 1/8 \\ [1.0769 - 0.2424(s/a)](d/b)^{p_2}, & 1/8 \leqslant s/a \leqslant 1/4 \end{cases} \tag{15}$$

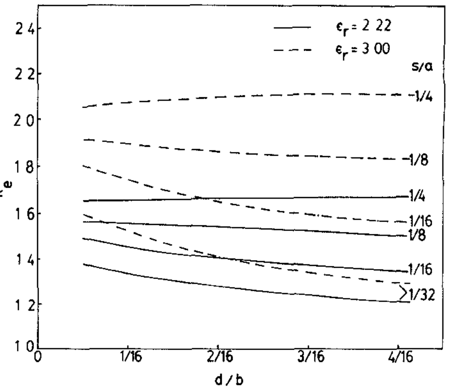

Fig. 4. Effective dielectric constant k_e in unilateral fin-lines. $b/a = 0.5$, $\epsilon_r = 2.22$ and 3, $b/\lambda = 0.3556$.

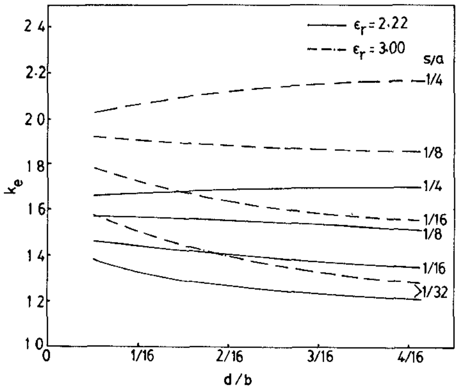

Fig. 5. Effective dielectric constant k_e in bilateral fin-lines. $b/a = 0.5$, $\epsilon_r = 2.22$ and 3, $b/\lambda = 0.3556$.

where

$$p_1 = 0.089 + 0.288(s/a)$$

$$p_2 = 0.16 - 0.28(s/a).$$

Figs. 4 and 5 show the typical values of k_e computed with the above expressions at $b/\lambda = 0.3556$.

VI. Characteristic Impedance

The characteristic impedance of the fin-line has been presented by Meier [1] in terms of the asymptotic value $Z_{0\infty}$ (2), that is, the impedance at infinite frequency of an equivalent ridged waveguide structure. This impedance can be defined in many different ways. The choice of the definition depends on the application. For instance, in Meier's expression (2), $Z_{0\infty}$ is defined on a power-voltage basis. However, Meinel and Rembold [10] have found that in the design of fin-line switches it is appropriate to define characteristic impedance in terms of a voltage and current, that is

$$Z_0 = \frac{V_0}{I_l} \tag{16}$$

where V_0 is the line integral over the electric field between the fins taken along the shortest path on the substrate surface, and I_l is the total longitudinal surface current in the structure. This definition was proposed by Hofmann [4].

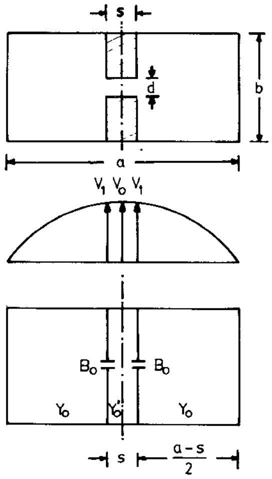

Fig. 6. Cross section of double-ridged waveguide with transverse equivalent network showing the voltage distribution.

In this section, we shall derive an analytical expression for the characteristic impedance of an equivalent ridged waveguide structure at infinite frequency. To that end, we shall calculate the total longitudinal current with a procedure similar to that of Cohn [11], taking into account the current on the edges of the ridge.

The longitudinal current is equal to the sum of the respective currents in the three regions of the double-ridged waveguide structure shown in Fig. 6. The transverse equivalent network and the voltage distribution in the TE_{10} mode are also shown there.

A. The Longitudinal Current Between the Ridges

(Region 1): Following the notation of Fig. 6, the voltage decreases cosinusoidally outwards from the center and can be expressed as

$$V(l) = V_0 \cos 2\pi l/\lambda_t \tag{17}$$

where V_0 is the magnitude of the voltage at the center, l is the variable distance from the center, and λ_t is the wavelength in the transverse direction, which is equivalent to the cutoff wavelength λ_{ca} of the air-filled ridged waveguide given by

$$\lambda_t = \lambda\left[1-(\lambda/\lambda_g)^2\right]^{-1/2} = \lambda_{ca}. \tag{18}$$

The voltage at the step is

$$V_1 = V_0 \cos \pi s/\lambda_{ca} \tag{19}$$

which is obtained setting $l = s/2$ in (17). Thus, the longitudinal linear current density at the top wall is

$$J(l) = \frac{V_0}{d\eta}\cos 2\pi l/\lambda_{ca} \tag{20}$$

where

$$\eta = \sqrt{\frac{\mu_0}{\epsilon_0}}\,\frac{\lambda_g}{\lambda} \tag{21}$$

is the characteristic wave impedance of the TE_{10} mode in the structure. The longitudinal current is then derived as

$$I_{l1} = \frac{2}{d}\int_0^{\frac{s}{2}} \frac{V_0}{\eta}\cos 2\pi l/\lambda_{ca}\, dl = \frac{V_0 \lambda_{ca}}{\pi \eta d}\sin \pi s/\lambda_{ca}. \tag{22}$$

B. The Longitudinal Current in the Discontinuity Plane

(Region 2): Assuming that the discontinuity region can be represented by a shunt capacitance C_s per unit length subject to the voltage

$$V_1 = V_0 \cos \pi s/\lambda_{ca} \tag{23}$$

we can imagine it as a parallel plate capacitor of plate distance h and width l in the transverse direction

$$C_s = \epsilon_0 l/h. \tag{24}$$

The electric field strength in the capacitor is then

$$E_c = V_1/h = \frac{V_0}{h}\cos \pi s/\lambda_{ca}. \tag{25}$$

The current in the top plate is

$$I_t = \frac{V_0 C_s}{\eta \epsilon_0}\cos \pi s/\lambda_{ca}. \tag{26}$$

The total discontinuity current, taking into account both halves of the cross section, is then

$$I_{l2} = \frac{2V_0}{\eta\omega\epsilon_0}\,\frac{\omega C_s}{Y_{0t}}\cdot Y_{0t}\cos \pi s/\lambda_{ca} \tag{27}$$

with

$$Y_{0t} = \frac{\epsilon_0}{\mu_0}\,\frac{1}{b}. \tag{28}$$

After some further modifications, this current becomes, for a finite real λ_g in the longitudinal direction

$$I_{l2} = \frac{V_0 \lambda_{ca}}{\pi \eta b}(B_0/Y_0)\cos \pi s/\lambda_{ca}. \tag{29}$$

The expression for B_0/Y_0 is presented later in (34).

C. The Longitudinal Current in the Lateral Parts

(Region 3): In the lateral parts of the cross section, the voltage variation in the transverse direction is

$$V(l) = V_0 \frac{\cos \pi s/\lambda_{ca}}{\sin \pi(a-s)/\lambda_{ca}}\sin 2\pi l/\lambda_{ca} \tag{30}$$

where l is now the variable distance inward from the side walls. The longitudinal current density in the top wall becomes

$$J(l) = \frac{V_0 \cos \pi s/\lambda_{ca}}{b\eta \sin \pi(a-s)/\lambda_{ca}}\sin 2\pi l/\lambda_{ca} \tag{31}$$

and the expression for longitudinal current is given by

$$I_{l3} = 2\int_0^{(a-s)/2} \frac{V_0 \cos \pi s/\lambda_{ca}}{b\eta \sin \pi(a-s)/\lambda_{ca}}\sin 2\pi l/\lambda_{ca}\, dl = \frac{V_0 \lambda_{ca}}{\pi \eta b}\cos(\pi s/\lambda_{ca})\tan\left[\pi(a-s)/2\lambda_{ca}\right]. \tag{32}$$

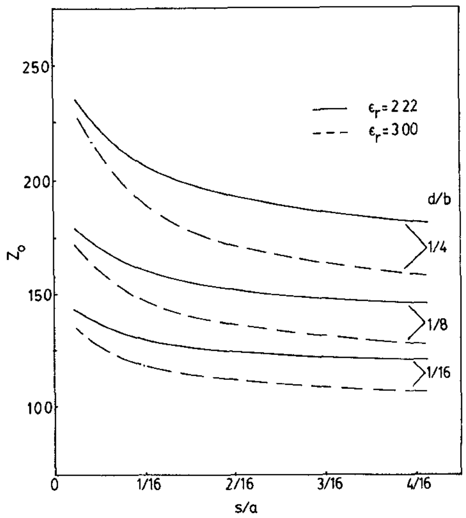

Fig. 7. Characteristic impedance of unilateral fin-lines. $b/a = 0.5$, $\epsilon_r =$ 2.22 and 3, $b/\lambda = 0.3556$.

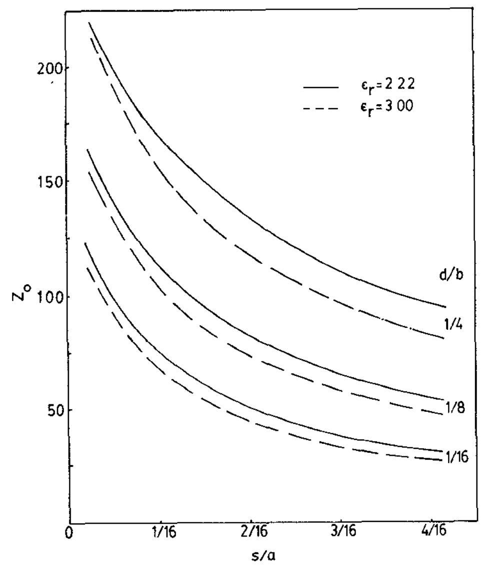

Fig. 8. Characteristic impedance of bilateral fin-lines. $b/a = 0.5$, $\epsilon_r =$ 2.22 and 3, $b/\lambda = 0.3556$.

With the three components of the total longitudinal current derived above, the characteristic impedance at infinite frequency is given by

$$Z_{0\infty VI} = \frac{120\pi^2(b/\lambda_{ca})}{\frac{b}{d}\sin\frac{\pi s}{\lambda_{ca}} + \left[\frac{B_0}{Y_0} + \tan\frac{\pi(a-s)}{2\lambda_{ca}}\right]\cos\frac{\pi s}{\lambda_{ca}}} \tag{33}$$

with

$$\frac{B_0}{Y_0} = \frac{2b}{\lambda_{ca}}\left\{\ln\csc\left(\frac{\pi d}{2b}\right) + \frac{Q\cos^4\left(\frac{\pi d}{2b}\right)}{1+Q\sin^4\left(\frac{\pi d}{2b}\right)} + \frac{1}{16}\left(\frac{b}{\lambda_{ca}}\right)^2\left[1-3\sin^2\left(\frac{\pi d}{2b}\right)\right]^2\cos^4\left(\frac{\pi d}{2b}\right)\right\} \tag{34}$$

and

$$Q = \left[1-(b/\lambda_{ca})^2\right]^{-1/2} - 1. \tag{35}$$

The characteristic impedance Z_0 is computed using (33) and (2). The value of s in (33) is set equal to zero in the case of unilateral fin-line, and it is set equal to the substrate thickness in the case of bilateral fin-line. Z_0 is shown in Figs. 7 and 8 for unilateral and bilateral fin lines as a function of s/a for various values of d/b at $b/\lambda = 0.3556$. These values agree within ± 2 percent with Hofmann's results [12].

VII. Results and Conclusions

In the foregoing sections, we have presented expressions for the evaluation of the cutoff wavelength, guided wavelength, and characteristic impedance of unilateral and bilateral fin-lines. These expressions are directly applicable to the design of fin-line circuits. The expressions for the cutoff wavelength agree within ± 1 percent and those of guided wavelength agree within ± 2 percent with the results obtained with the spectral domain technique. These expressions may look slightly complicated at a first glance, but when applied to a practical problem, they reduce to a very simple expression of the form $y = Ax^B$. This is so because the designer initially fixes the thickness of the substrate and chooses a given waveguide size, thus fixing the values of b/a and s/a. The only remaining variable parameter is then the normalized gap width d/b. The expression for the characteristic impedance agrees also within ± 2 percent with the values given by Hofmann [12]. This definition of characteristic impedance is appropriate in impedance matching problems and in the characterization of discontinuities in fin-line structures [13].

References

[1] P. J. Meier, "Integrated fin-line millimeter components," *IEEE Trans. Microwave Theory Tech.*, vol. MTT-22, pp. 1209–1216, Dec. 1974.

[2] A. M. K. Saad and G. Begemann, "Electrical performance of fin-lines of various configurations," *Microwaves, Opt. Acoust.*, vol. 1, pp. 81–88, Jan. 1977.

[3] W. J. R. Hoefer, "Fin-line design made easy," in 1978 IEEE MTT-S Int. Microwave Symp., (Ottawa, Canada), p. 471.

[4] H. Hofmann, "Dispersion of planar waveguides for millimeter-wave applications," *Arch. Elek. Ubertragung.*, vol. 31, pp. 40–44, Jan. 1977.

[5] J. B. Knorr and P. M. Shayda, "Millimeter-wave fin-line characteristics," *IEEE Trans. Microwave Theory Tech.*, vol. MTT-28, pp. 737–743, July 1980.

[6] L.-P. Schmidt and T. Itoh, "Spectral domain analysis of dominant and higher order modes in fin-lines," *IEEE Trans. Microwave Theory Tech.*, vol. MTT-28, pp. 981–985, Sept. 1980.

[7] A. Beyer and I. Wolff, "A solution of the earthed fin-line with finite metallization thickness," in *1980 IEEE MTT-S Int. Microwave Symp. Dig.*, (Washington, DC), pp. 258–260.

[8] A. K. Sharma and W. J. R. Hoefer, "Empirical analytical expressions for the fin-line design," in *1981 IEEE MTT-S Int. Microwave Symp. Dig.*, (Los Angeles, CA), pp. 102–104.

[9] A. K. Sharma, G. I. Costache, and W. J. R. Hoefer, "Cutoff in fin-lines evaluated with the spectral domain technique and with the finite element method," in *1981 IEEE AP-S Int. Antenna Propagation Symp. Dig.*, (Los Angeles, CA), pp. 308–311.

[10] H. Meinel and B. Rembold, "New millimeter-wave fin-line attenuators and switches," in *1979 IEEE MTT-S Int. Microwave Symp. Dig.*, (Orlando, FL), pp. 249–252.

[11] S. B. Cohn, "Properties of ridge waveguide," *Proc. IRE*, vol. 35, pp. 783–788, Aug. 1947.
[12] H. Hofmann, private communication.
[13] E. Pic and W. J. R. Hoefer, "Experimental characterization of fin-line discontinuities using resonant techniques," in *1981 IEEE MTT-S Int. Microwave Symp. Dig.*, (Los Angeles, CA), pp. 108–110.

Arvind K. Sharma (S'74–M'80) was born in Jodhpur, Rajasthan, India, on December 4, 1951. He received the B.E. (Hons.) degree in electronics from Birla Institute of Technology and Science, Pilani, Rajasthan, in 1973, and the M. Tech. degree in electronics and communication engineering, and the Ph.D. degree from the Indian Institute of Technology, Delhi, in 1975 and 1981, respectively.

From 1980–1982, he was with the Department of Electrical Engineering, University of Ottawa, Ottawa, Ontario, Canada, as a Research Associate. Since 1982 he has been with the Microwave Technology Center, RCA Laboratories, David Sarnoff Research Center, Princeton, NJ. His areas of research interest include microwave and millimeter-wave integrated circuits, and analytical and numerical methods in electromagnetics.

Dr. Sharma received the Best Paper Award in the Student Paper Contest organized by the IEEE India Section in 1975. He was awarded the IEEE Outstanding Student Member Award in 1975.

Wolfgang J. R. Hoefer (M'71–SM'78) was born in Urmitz/Rhein, Germany, on February 6, 1941. He received the diploma in electrical engineering from the Technische Hochschule Aachen, Aachen, Germany, in 1964, and the D. Ing. degree from the University of Grenoble, Grenoble, France, in 1968.

After one year of teaching and research at the Institut Universitaire de Technologie, Grenoble, France, he joined the Department of Electrical Engineering, the University of Ottawa, Ottawa, Ontario, Canada where he is currently a Professor. During a sabbatical year in 1976–1977, he spent six months with the Space Division of the AEG-Telefunken in Backnang, Germany, and six months with the Institut National Polytechnique de Grenoble, France. His research interests include microwave measurement techniques, millimeter-wave circuit design, and numerical techniques for solving electromagnetic problems.

Dr. Hoefer is a registered Professional Engineer in the province of Ontario, Canada.

Short Papers

A Quasi-Optical Nulling Method for Material Birefringence Measurements at Near-Millimeter Wavelengths

GEORGE J. SIMONIS, MEMBER, IEEE

Abstract —**A quasi-optical technique for the measurement of birefringence is demonstrated at 245 GHz. The technique is applied to crystal quartz. The measured values are compared with values reported at nearby frequencies. The technique is used to determine the difference between the ordinary and extraordinary real indices of refraction directly, rather than by deducing the difference from separate measurements of the two indices. The technique is based on establishing a transmission null, thus providing appreciable sensitivity and precision for the measurement.**

I. Introduction

In the infrared wavelength range, many conventional optical techniques are employed for materials characterization. In the microwave region, fundamental mode waveguide and microwave discrete-frequency sources are brought to bear on the problem with the material of interest often completely filling a section of the waveguide. The near-millimeter-wave region (NMMW—approximately 94 to 1000 GHz) presents particular problems and warrants somewhat specialized approaches. The wavelength is large enough that diffraction effects can be a substantial perturbation to "optical" configurations. The wavelength is small enough that the small waveguide is difficult to work with and to uniformly fill with the sample material. An NMMW technique is described here that employs a quasi-optical configuration to measure sample birefringence directly, without first measuring the magnitudes of the individual indices.

The radiation source is a CO_2-laser-pumped metal-waveguide $C^{13}H_3F$ laser 2 m long emitting at 1.222-mm wavelength (245 GHz). The average power available is much less than 1 mW, but is quite sufficient to provide a good signal-to-noise ratio for the measurements. Such sources typically undergo substantial amplitude fluctuations, but have good frequency stability, operating within a few megahertz of the gain line center of the lasing gas. The optics and sample dimensions are kept greater than 1 in in clear aperature in order to reduce diffraction effects. The source and experiment are isolated in this work by an absorption "pad" in the optical path.

The critical elements in the configuration are wire grating polarizers made at Harry Diamond Laboratories. They are made using a machine shop lathe in an approach [1] similar in some

Manuscript received June 25, 1982; revised November 22, 1982.
The author is with the Army Electronics Research and Development Command, Harry Diamond Laboratories, 2800 Powder Mill Road, Adelphi, MD 20783.